



.....

## A STUDY ON MULTI-OBJECTIVE OPTIMIZATION OF PLUNGE CENTERLESS GRINDING PROCESS

Phan Bui Khoi<sup>a</sup>, Do Duc Trung<sup>b,\*</sup>, Ngo Cuong<sup>b</sup>

<sup>a</sup>School of Mechanical Engineering, Hanoi University of Science and Technology,  
No. 1, Dai Co Viet, Hanoi, Viet Nam

<sup>b</sup>College of Economics and Technology, Thai Nguyen University Group 15,  
Thinh Dan Ward, Thai Nguyen City, Viet Nam

### ABSTRACT

Round component with the minimum value of surface roughness and roundness error is the goal of most of the fine machine processes. This paper presents the research on optimization of plunge centerless grinding process when grinding the 20X-carbon infiltration steel (ГОСТ standard - Russia) to achieve the minimum value of surface roughness and roundness errors. The input parameters are center height angle of the workpiece ( $\beta$ ), longitudinal dressing feed-rate ( $S_{sd}$ ), plunge feed-rate ( $S_k$ ) and control wheel velocity ( $v_{ad}$ ) using the result of 29 sets in central composite design matrix to show the two second orders of surface roughness and roundness error models. The final goal of this work focuses on the determination of optimum centerless grinding above the parameters for the minimization of surface roughness ( $Ra_{min} = 0,3090\mu m$ ) and roundness errors ( $\Delta_{min} = 1,3493\mu m$ ).

**Keywords:** Plunge Centerless Grinding, Optimization, Surface Roughness, Roundness Error.

### 1. INTRODUCTION

Centerless grinding is widely used in industry for precision machining of cylindrical components because of its high production rate, easy automation, and high accuracy. 20X - carbon infiltration steel is a common alloy steel that is usually used in mechanical engineering using centerless grinding process.

To improve the centerless grinding process, it is necessary to optimize surface roughness and roundness errors, the most critical quality constraints for the selection of grinding factors in process planning.

Researches on the optimization of centerless grinding process were published by many authors: Minimizing the surface roughness and roundness errors of workpiece by selecting the optimization levels of control wheel speed, feed rate and depth of cut [1]. Minimizing the roundness error of workpiece and carrying out the regression analysis to model an equation to average out roundness error [2]. Predicting the set-up conditions to analyze the dynamic and geometrical instabilities, making it possible to study the influence of different machine variables in stability of the process [3]. Minimizing the surface roughness by developing an empirical model for it [4]. Minimizing the lobing effect by developing a stability diagram for workpiece and thereby selecting the grinding parameters and having found out that the characteristic root distribution of the lobing loop is periodic [5]. Investigating the workpiece roundness based on process parameters by both simulation and experimental analysis and finding out that a slower worktable feed rate and a faster workpiece rotational speed result in better roundness error [6]. Minimizing the roundness error of workpiece by selecting the optimization levels of dressing feed, grinding feed, dwell time and cycle time [7]. Minimizing the roundness error of workpiece by selecting the optimization range of the center height angle [8]. Giving a method of how to select the optimal stable geometrical configuration in centerless grinding [9]. Giving an algorithm for providing the optimum set-up condition [10]., etc.

This paper presents the research on the optimization of plunge centerless grinding process when grinding the 20X-carbon infiltration steel to achieve the minimum value of surface roughness and roundness errors. The input parameters include center height angle of the workpiece ( $\beta$ ), longitudinal dressing feed-rate ( $S_{sd}$ ), plunge feed-rate ( $S_k$ ) and control wheel velocity ( $v_{dd}$ ).

## 2. EXPERIMENT SYSTEM

### 2.1. Centerless grinding model

Plunge centerless grinding model is illustrated in figure 1. The value of center height angle ( $\beta$ ) can be adjusted by the value of A. The relationship between ( $\beta$ ) and A in equation 1 is:

$$\beta = \arcsin\left(\frac{A - R_{ct} - H}{R_{dm} + R_{ct}}\right) + \arcsin\left(\frac{A - R_{ct} - H}{R_{dd} + R_{ct}}\right) \quad (1)$$

Where, H is the distance from the grinding wheel center, control wheel center to the bottom of the workrest blade.

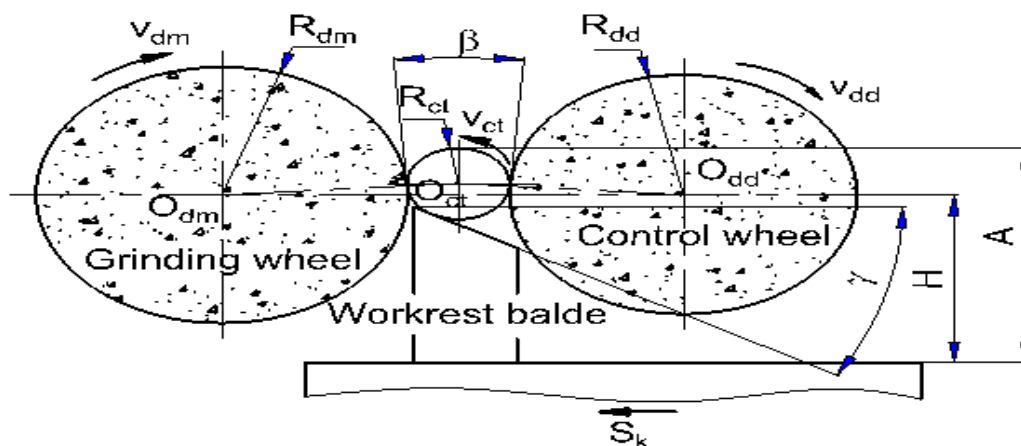


Fig 1: Plunge centerless grinding model

### 2.2. Components

The component material was the 20X-carbon infiltration steel (62HRC), applied to the serial production elements for diesel engine and attachments. The experimental component, shown in Fig 2, was supported by specially made workrest blade with a 30° angle. The chemical composition of experimental component is in Table 1.

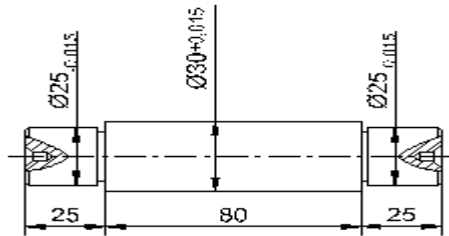


Fig 2: Experimental component

Table 1: Chemical composition of experimental component

C(%)	Si(%)	Mn(%)	P(%)	S(%)	Cr(%)	Ni(%)	Cu(%)
1,02	0,212	0,51	0,018	0,017	0,78	0,017	0,021

### 2.3. Grinding wheels

Using the Al<sub>2</sub>O<sub>3</sub> grinding wheel of Hai Duong Grinding Wheels Joint Stock Company, Viet Nam, Cn80.TB<sub>1</sub>.G.V<sub>1</sub>.500.150.305x35m/s.

Besides, the standard rubber bonded control wheel of 273 mm x 150 mm x 127 mm dimensions was employed.

### 2.4. Experimental machine tool

The grinding experiments were conducted on a M1080B centerless grinder with H = 210 mm, shown in Fig 3.



Fig 3: Experimental machine tool

### 2.4. Measuring equipment

The surface roughness was measured by a Mitutoyo Surftest SJ-401 at 0,8 mm cutoff value. The roundness error was measured by a dial gage with a precision of 5/10.000. Each ground component was measured three times. The surface roughness and roundness error response, summarized in Table 2, are the average reading of three consecutive measurements.

### 3. EXPERIMENT MATRIX

The experiment matrix was conducted under chatter free conditions to keep the grinding wheel speed (34 m/s), the grinding depth (0,05 mm), the depth of dressing (0,01 mm), the spark-out time (1 s) and the coolant flow constant.

In this work, using the central composite design with four input parameters ( $\beta$ ,  $S_{sd}$ ,  $S_k$ ,  $v_{dd}$ ), their levels are presented in Table 2. This experimental matrix with 29 sets; these sets include 16 single-replicated orthogonal factorial points, 8 axial points located and 5 centre points, shown in Table 3.

**Table 2:** Input parameters and theirs levels

Input parameters	Symbol	Parameter levels				
		-2	-1	0	1	2
Center height angle ( $^\circ$ )	$\beta$	4,8	6,0	7,2	8,4	9,6
Dressing feed-rate (mm/min)	$S_{sd}$	100	200	300	400	500
In-feed speed ( $\mu\text{m/s}$ )	$S_k$	2	6	10	14	18
Control wheel velocity (m/min)	$v_{dd}$	18,9	24,25	29,6	34,95	40,3

**Table 3:** Experimental matrix

Set	$\beta$	$S_{sd}$	$S_k$	$v_{dd}$	$R_a (\mu\text{m})$	$R_a^* (\mu\text{m})$	$\Delta (\mu\text{m})$	$\Delta^* (\mu\text{m})$
1	1	-1	-1	1	0.44	0.42	2,67	2.84
2	0	0	-2	0	0.69	0.69	2,33	2.11
3	-2	0	0	0	0.91	0.90	2,50	2.28
4	-1	1	-1	-1	1.26	1.27	3,33	3.46
5	-1	1	-1	1	1.01	1.02	2,67	2.81
6	0	0	0	0	0.42	0.41	1,00	1.23
7	-1	-1	1	-1	0.52	0.52	2,50	2.58
8	1	-1	1	1	0.58	0.58	3,00	3.05
9	-1	-1	-1	-1	0.51	0.51	2,17	2.29
10	1	1	1	1	0.73	0.73	1,00	1.15
11	0	0	0	-2	0.64	0.63	3,33	3.14
12	-1	-1	1	1	0.48	0.47	1,83	2.00
13	-1	1	1	-1	1.12	1.14	2,67	2.76
14	1	1	1	-1	1.02	1.03	1,17	1.30
15	0	0	0	0	0.40	0.41	1,33	1.23
16	0	0	0	0	0.42	0.41	1,00	1.23
17	0	0	0	0	0.39	0.41	1,33	1.23
18	0	0	0	2	0.40	0.40	3,33	3.08
19	1	-1	-1	-1	0.29	0.29	1,50	1.58
20	1	-1	1	-1	0.57	0.56	2,33	2.45
21	1	1	-1	1	0.70	0.71	1,83	1.94
22	-1	-1	-1	1	0.57	0.57	2,33	2.38
23	-1	1	1	1	0.77	0.78	1,33	1.44
24	2	0	0	0	0.63	0.64	1,50	1.28
25	0	2	0	0	1.35	1.32	2,00	1.75
26	0	-2	0	0	0.39	0.41	2,67	2.48
27	1	1	-1	-1	0.89	0.89	1,33	1.42
28	0	0	2	0	0.73	0.73	1,83	1.61
29	0	0	0	0	0.44	0.41	1,50	1.23

### 3. EFFECT OF INPUT PARAMETERS ON OUTPUT PARAMETERS

#### 3.1. Effect of input parameters on surface roughness

Fig 4 depicts the main effect on surface roughness. The interaction effect of input parameters on surface roughness are shown in Figs 5-10. In each of these graphs, two input parameters are varied while the third and fourth parameters are the help as its mid value. The graphs show that all of the input parameters have a significant effect on the surface roughness.

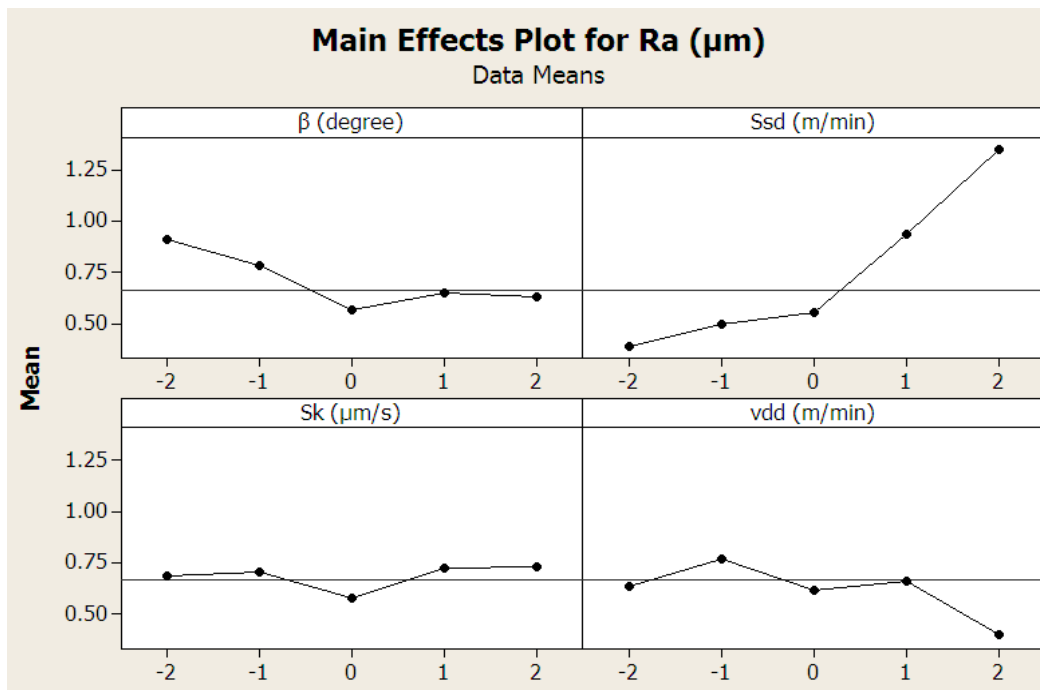


Fig 4: Main effect of input parameters on Ra

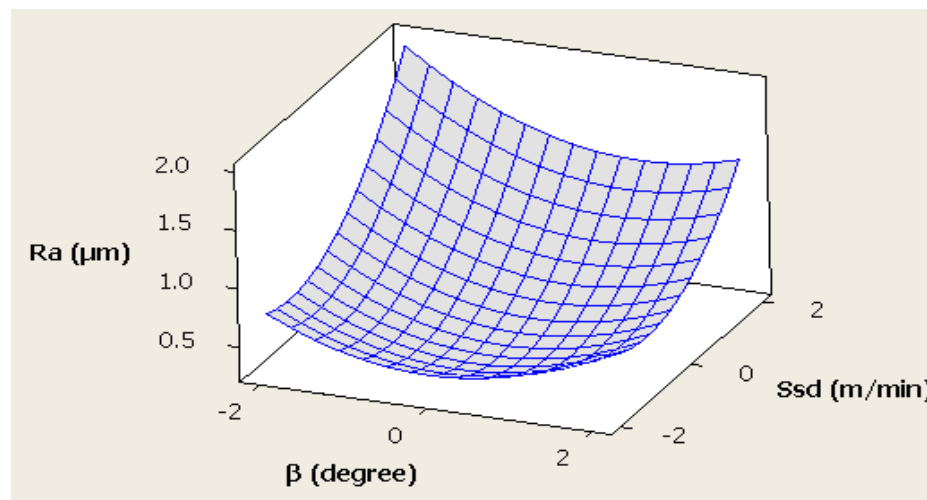


Fig 5: Interaction effect of  $\beta$  and  $S_{sd}$  on Ra

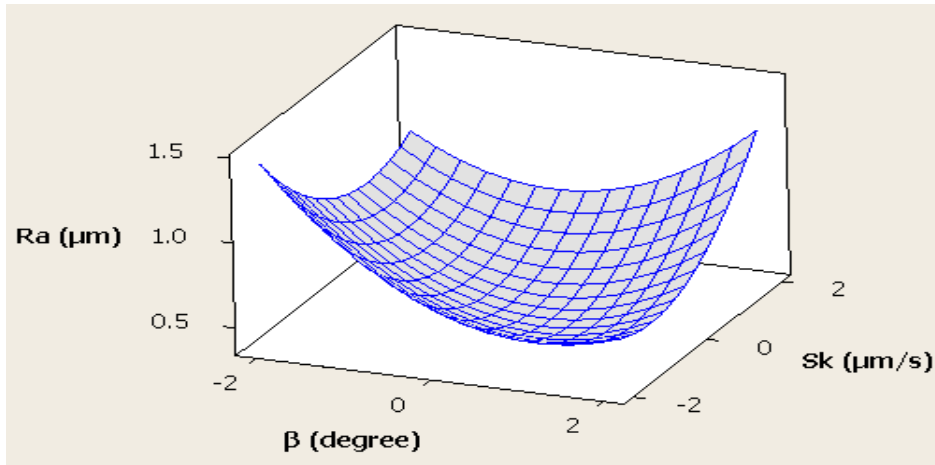


Fig 6: Interaction effect of  $\beta$  and  $S_k$  on  $R_a$

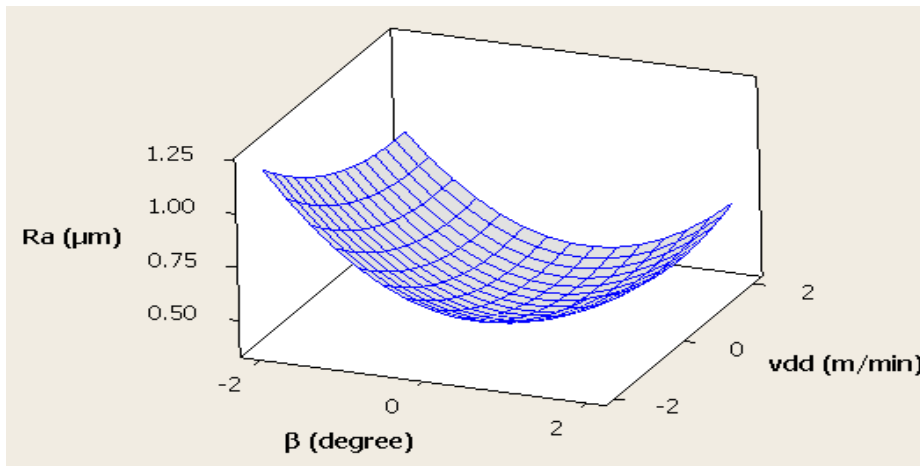


Fig 7: Interaction effect of  $\beta$  and  $v_{dd}$  on  $R_a$

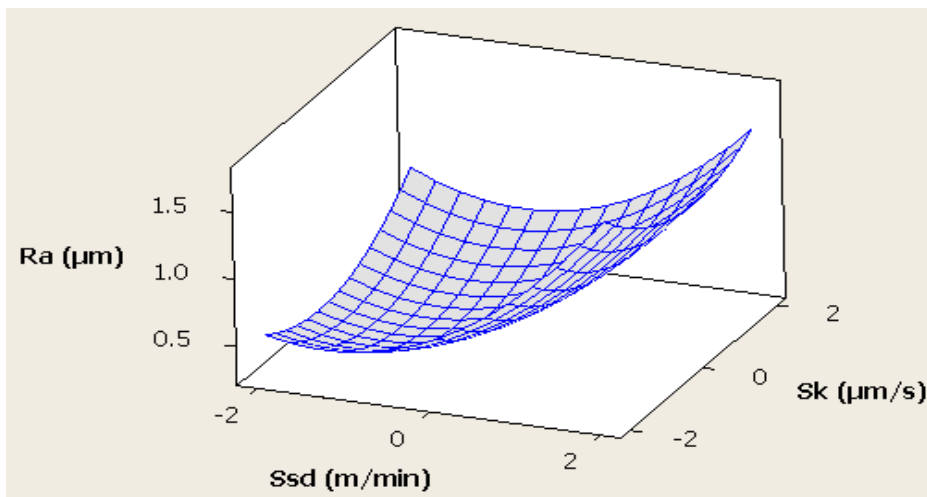


Fig 8: Interaction effect of  $S_{sd}$  and  $S_k$  on  $R_a$

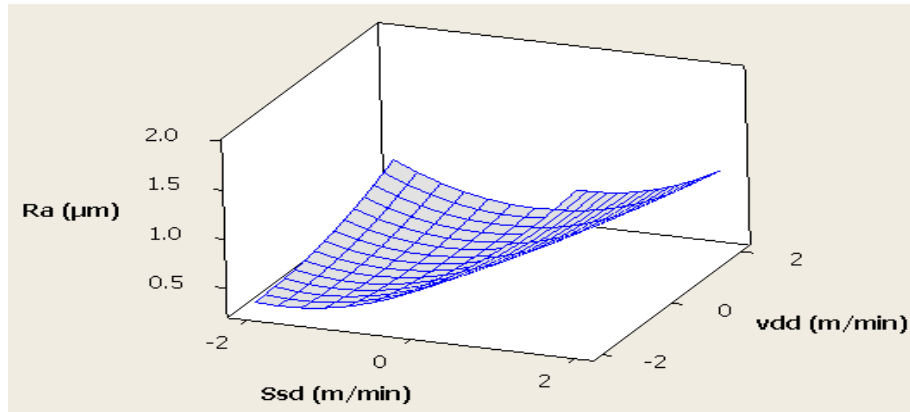


Fig 9: Interaction effect of  $S_{sd}$  and  $v_{dd}$  on  $Ra$

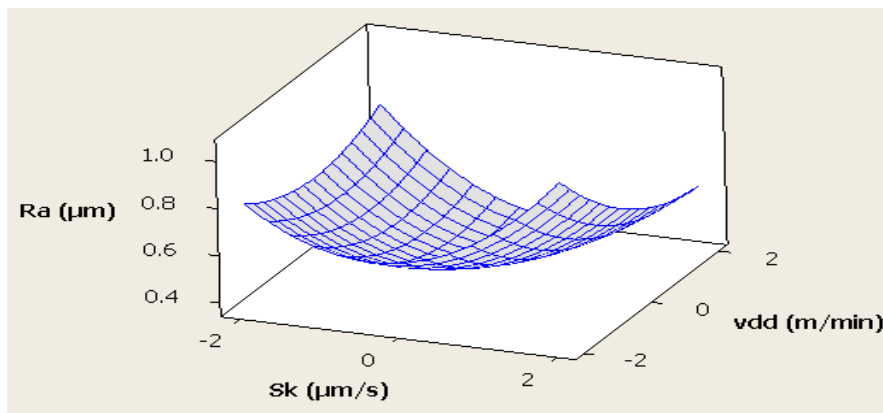


Fig 10: Interaction effect of  $S_k$  and  $v_{dd}$  on  $Ra$

### 3.2. Effect of input parameters on roundness error

Fig 11 depicts the main effect on roundness error. The interaction effect of input parameters on surface roughness are shown in Figs 12-17. In each of these graphs, two input parameters are varied while the third and fourth parameters are the help as its mid value. The graphs show that all of the input parameters have a significant effect on the roundness error.

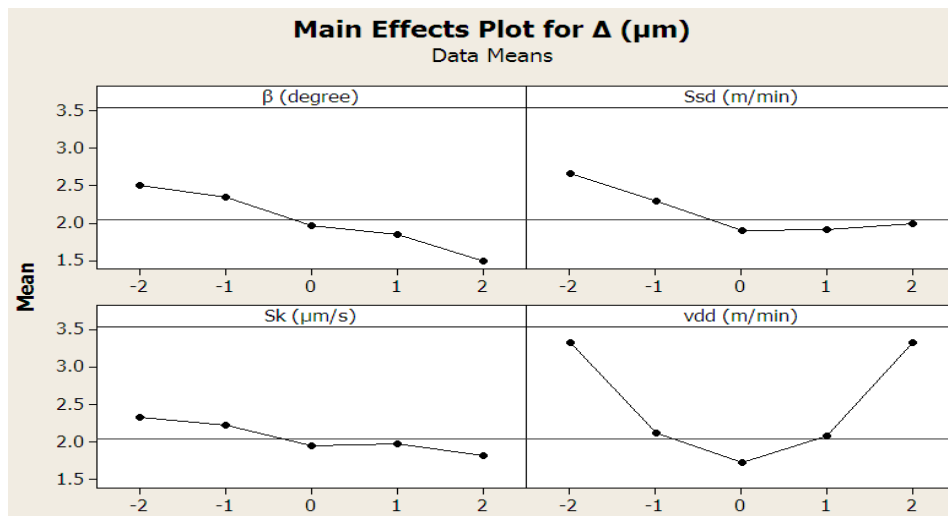


Fig 11: Main effect of input parameters on  $\Delta$

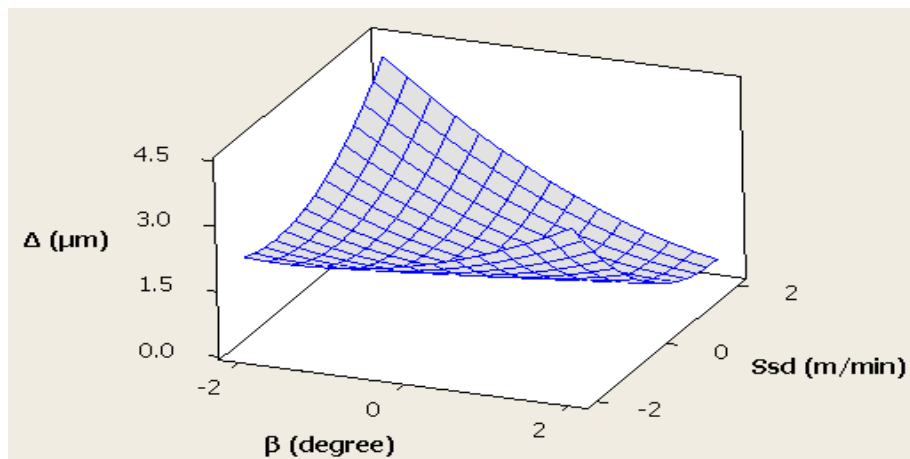


Fig 12: Interaction effect of  $\beta$  and  $S_{sd}$  on  $\Delta$

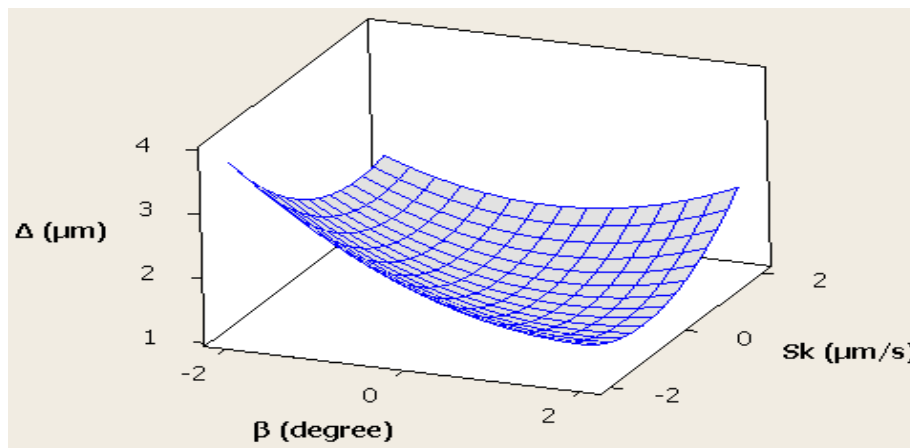


Fig 13: Interaction effect of  $\beta$  and  $S_k$  on  $\Delta$

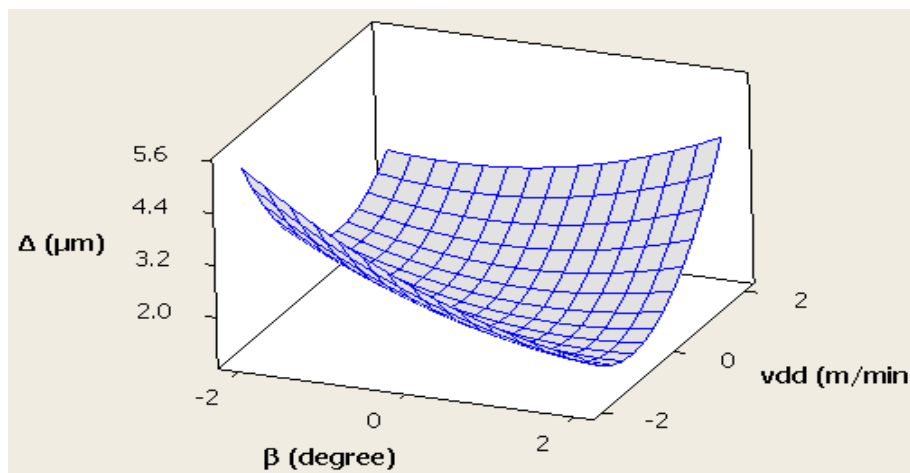


Fig 14: Interaction effect of  $\beta$  and  $v_{dd}$  on  $\Delta$



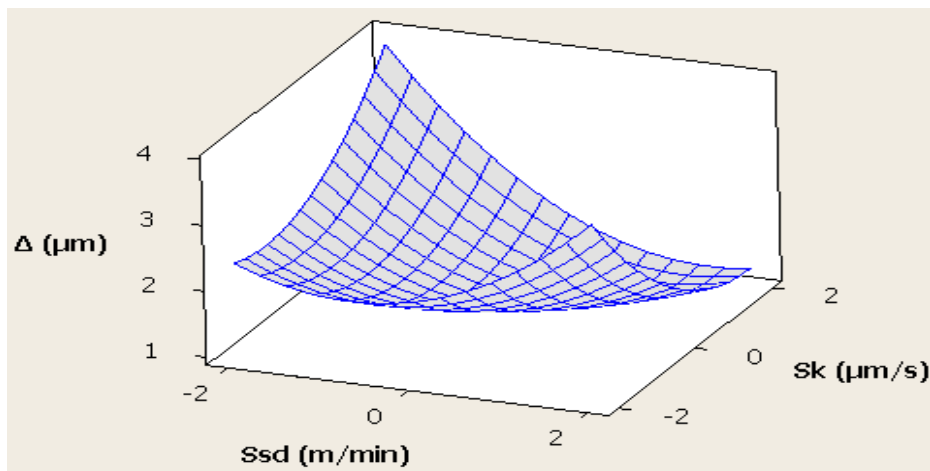


Fig 15: Interaction effect of  $S_{sd}$  and  $S_k$  on  $\Delta$

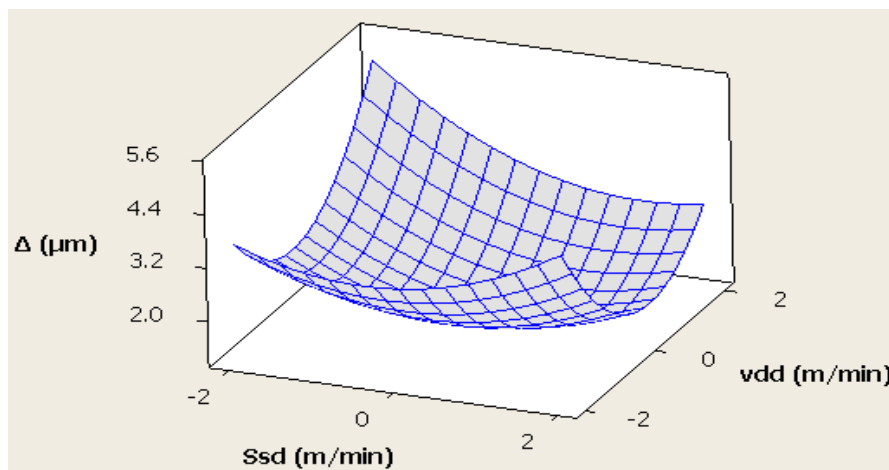


Fig 16: Interaction effect of  $S_{sd}$  and  $v_{dd}$  on  $\Delta$

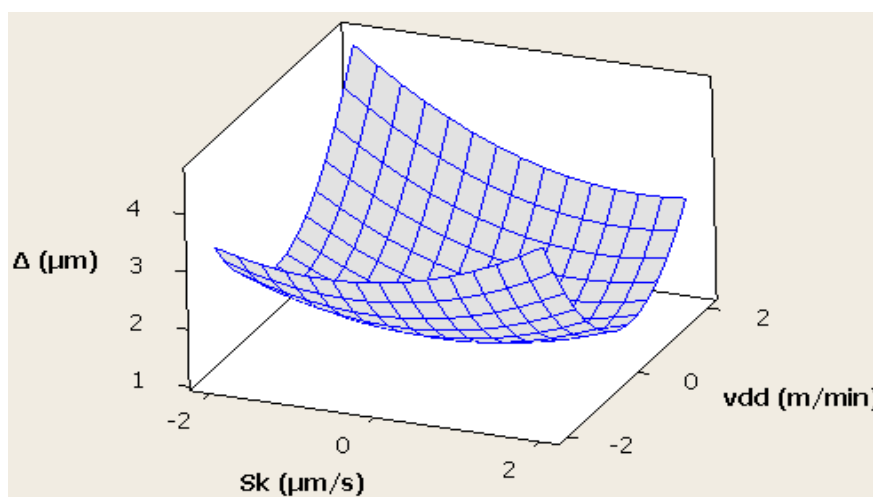


Fig 17: Interaction effect of  $S_k$  and  $v_{dd}$  on  $\Delta$

### 5. REGRESSION MODELS

The statistical analysis software Minitab 16 was used to determine the regression coefficients. The analysis for estimated regression coefficients for  $Ra$  and  $\Delta$  quadratic models is shown in Tables 4 and 5 respectively. The surface roughness and roundness error models was developed in the form of non-reduced final equation in terms of coded parameters.

**Table 4:** Estimated regression coefficients for  $Ra$  quadratic model

Estimated Regression Coefficients for Ra				
Term	Coef	SE Coef	T	P
Constant	0.414000	0.007695	53.801	0.000
$\beta$	-0.065833	0.003512	-18.744	0.000
$S_{sd}$	0.227500	0.003512	64.772	0.000
$S_k$	0.008333	0.003512	2.373	0.033
$v_{dd}$	-0.057500	0.003512	-16.371	0.000
$\beta^2$	0.088792	0.003378	26.285	0.000
$S_{sd} \cdot S_{sd}$	0.113792	0.003378	33.686	0.000
$S_k \cdot S_k$	0.073792	0.003378	21.845	0.000
$v_{dd} \cdot v_{dd}$	0.026292	0.003378	7.783	0.000
$\beta \cdot S_{sd}$	-0.038750	0.004302	-9.008	0.000
$\beta \cdot S_k$	0.065000	0.004302	15.110	0.000
$\beta \cdot v_{dd}$	0.016250	0.004302	3.778	0.002
$S_{sd} \cdot S_k$	-0.035000	0.004302	-8.136	0.000
$S_{sd} \cdot v_{dd}$	-0.078750	0.004302	-18.307	0.000
$S_k \cdot v_{dd}$	-0.027500	0.004302	-6.393	0.000

$$\begin{aligned}
 Ra = & 0,4140 - 0,065833\beta + 0,22750S_{sd} + 0,008333S_k \\
 & - 0,0575v_{dd} + 0,088792\beta^2 + 0,113792S_{sd}^2 + 0,073792S_k^2 \\
 & + 0,026292v_{dd}^2 - 0,03875\beta \cdot S_{sd} + 0,065\beta \cdot S_k + 0,01625\beta \cdot v_{dd} \\
 & - 0,035S_{sd} \cdot S_k - 0,07875S_{sd} \cdot v_{dd} - 0,0275S_k \cdot v_{dd}
 \end{aligned}
 \tag{2}$$

**Table 5.** Estimated regression coefficients for  $\Delta$  quadratic model

Estimated Regression Coefficients for $\Delta$				
Term	Coef	SE Coef	T	P
Constant	1.23200	0.10776	11.432	0.000
$\beta$	-0.25000	0.04919	-5.083	0.000
$S_{sd}$	-0.18083	0.04919	-3.676	0.002
$S_k$	-0.12500	0.04919	-2.541	0.024
$v_{dd}$	-0.01417	0.04919	-0.288	0.778
$\beta^2$	0.13658	0.04731	2.887	0.012
$S_{sd} \cdot S_{sd}$	0.22033	0.04731	4.657	0.000
$S_k \cdot S_k$	0.15658	0.04731	3.310	0.005
$v_{dd} \cdot v_{dd}$	0.46908	0.04731	9.916	0.000
$\beta \cdot S_{sd}$	-0.33375	0.06024	-5.540	0.000
$\beta \cdot S_k$	0.14625	0.06024	2.428	0.029
$\beta \cdot v_{dd}$	0.29250	0.06024	4.855	0.000
$S_{sd} \cdot S_k$	-0.24875	0.06024	-4.129	0.001
$S_{sd} \cdot v_{dd}$	-0.18750	0.06024	-3.112	0.008
$S_k \cdot v_{dd}$	-0.16750	0.06024	-2.780	0.015

$$\begin{aligned} \Delta = & 1,232 - 0,25\beta - 0,18083S_{sd} - 0,125S_k - 0,014167v_{dd} \\ & + 0,13658\beta^2 + 0,22033S_{sd}^2 + 0,15658S_k^2 + 0,46908v_{dd}^2 \\ & - 0,33375\beta.S_{sd} + 0,14625\beta.S_k + 0,2925\beta.v_{dd} - 0,24875S_{sd}S_k \\ & - 0,1875S_{sd}v_{dd} - 0,1675S_kv_{dd} \end{aligned} \quad (3)$$

The upper models can be used to predict surface roughness and roundness error at particular design points. The numerical values of predicted responses  $R_a^*$  and  $\Delta^*$  are also summarized in Table 3. The differences between the measured and predicted responses are shown in Figs 18 and 19.

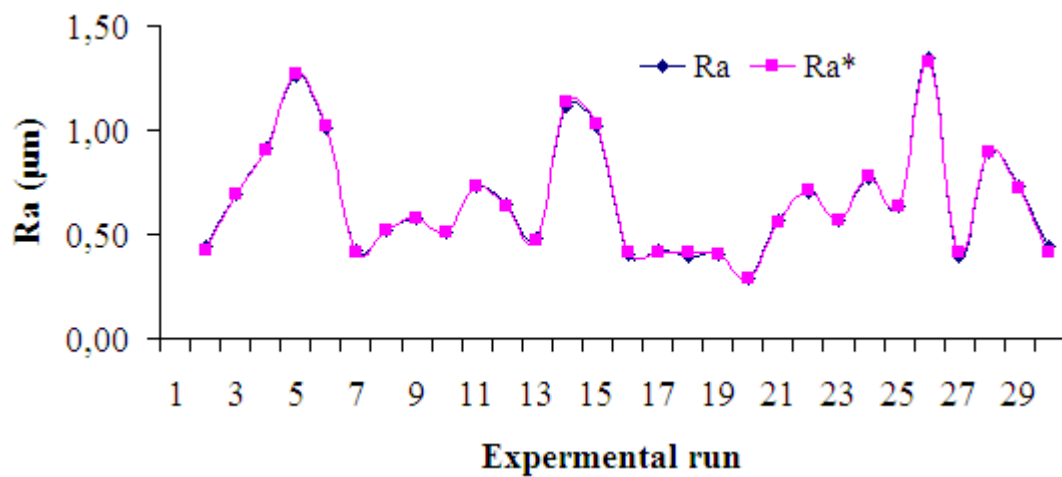


Fig 18: Measured and predicted surface roughness

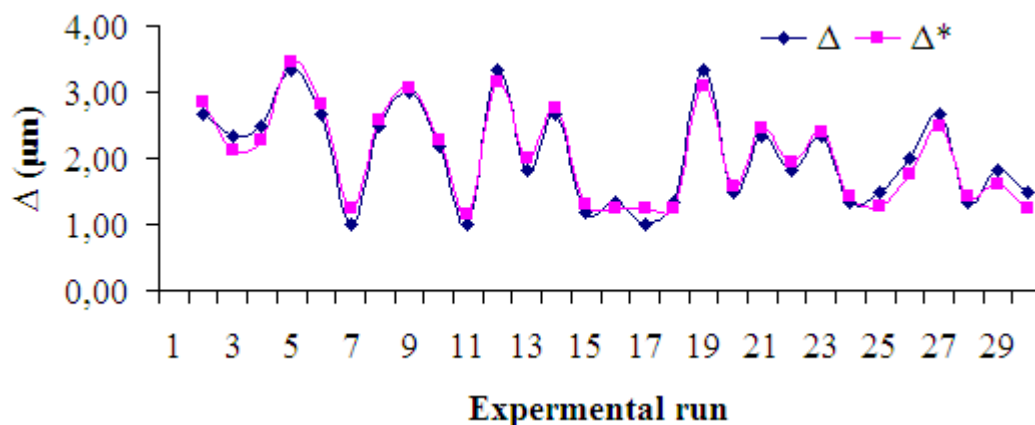


Fig 19: Measured and predicted roundness error

## 6. OPTIMIZATION

In the process of optimization, the goal is to minimize the surface roughness (Ra) and the roundness error ( $\Delta$ ), which form the multi objective optimization problem. Minitab 16 software is used to optimize these objectives. The optimization graph and numerical values are shown in Figure 20 and Table 6 respectively.

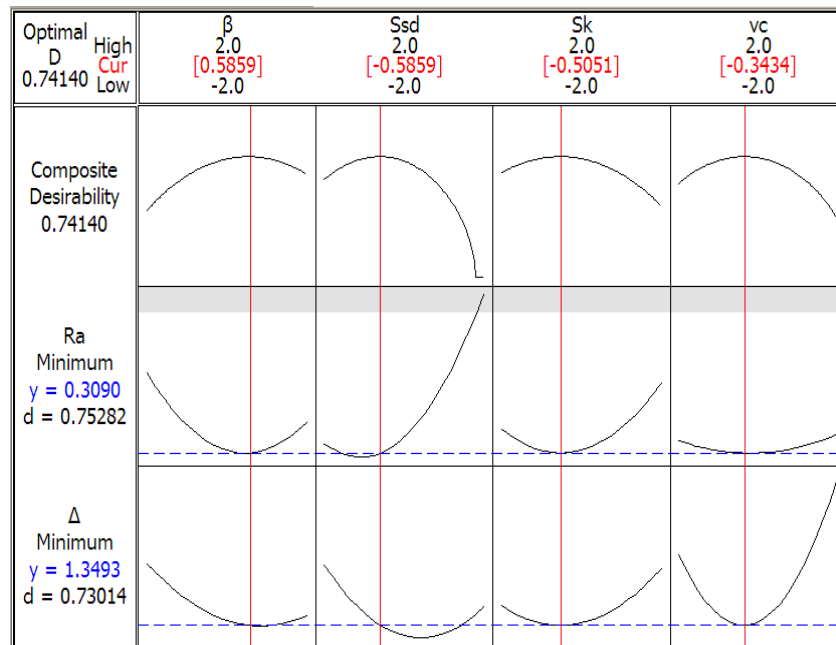


Fig 20: Optimization graph

Table 6: Optimization result

Output parameters	Objective function	Optimal input parameters				Predicted response
		$\beta$ ( $^\circ$ )	$S_{sd}$ (mm/min)	$S_k$ ( $\mu$ m/s)	$v_{dd}$ (m/min)	
Ra ( $\mu$ m)	Min	7,90	241,41	7,98	27,76	0,3090
$\Delta$ ( $\mu$ m)	Min					1,3493

## 7. CONCLUSION

For the work material 20X-carbon infiltration steel, all of four input parameters ( $\beta$ ,  $S_{sd}$ ,  $S_k$ ,  $v_{dd}$ ) have a significant effect on both output parameters, surface roughness and roundness error. Thus, to achieve the minimum surface roughness and roundness error of the 20X-carbon infiltration steel, the numerical values of  $\beta$ ,  $S_{sd}$ ,  $S_k$  and  $v_{dd}$  are  $7,9^\circ$ ; 241,41mm/min; 7,98 $\mu$ m/s and 27,76m/min respectively.

## REFERENCES

- [1] Senthil Kumar N, Dhinakarraj C K, Deepanraj and Sankaranarayyanan G (2012) Multi Objective Optimization and Empirical Modeling of centerless Grinding Parameters. Emerging Trends in Science, Engineering and Technology Lecture Notes in Mechanical Engineering 2012, pp 285-295.
- [2] Dhavlikar MN, Kulkarni MS, Mariappan V (2003) Combined Taguchi and dual response method for optimization of a centerless grinding operation. Int J Mater Process Technol 132:90–94.
- [3] Garitaonandia I, Fernandes MH, Albizuri J, Hernandez JM, Barrenetxe D (2010) A new perspective on the stability study of centerless grinding process. Int J Mach Tools Manuf 50:165–173.
- [4] Krajnik P, Kopac J, Sluga A (2005) Design of grinding factors based on response surface methodology. Int J Mater Process Technol 162–163:629–636.
- [5] Zhou SS, Gartner JR, Howes TD (1996) On the relationship between setup parameters and lobing behavior in centerless grinding. Ann CIRP 45(1):341–346.

- [6] Xu W, Wu Y, Sato T, Lin W (2010) Effects of process parameters on workpiece roundness in tangential-feed centerless grinding using a surface grinder. *Int J Mater Process Technol* 210:759–766.
- [7] Khan ZA, Siddiquee AN and Kamaruddin S (2012) Optimization of In-feed Centerless Cylindrica; Process Parameters Using Grey Relational Analysis. *Pertanika J Sci & Technol* 20(2): 257 – 268.
- [8] Subramanya Udupa NG, Shunmagam MS and Radhakrishman V (1987) Optimizing workpiece position in centerless grinding by roundness profile analysis. *Butter & Co (Publishers) Ltd*: 23-30.
- [9] Chien AY (1984) The Selection of Optimal Stable Geometrical Configuration in Centerless Grinding. *Int J. Mach Tool. Des. Res Vol 24 No 2*: 87-93.
- [10] Hashimoto F, Kanai A and Miyshita M (2004) Optimisation of Set-Up Conditions of the Centerless Grinding Process. *Ann. CIRP* 53 (1) 271-274.
- [11] Vishal Francis, Abhishekkhalkho, Jagdeptirkey, Rohit Silas Tigga and Neelamanmoltirkey, “Experimental Investigation and Prediction of Surface Roughness in Surface Grinding Operation using Factorial Method and Regression Analysis”, *International Journal of Mechanical Engineering & Technology (IJMET)*, Volume 5, Issue 5, 2014, pp. 108 - 114, ISSN Print: 0976 – 6340, ISSN Online: 0976 – 6359.
- [12] Gunwant D.Shelake, Harshal K. chavan, Prof. R. R. Deshmukh and Dr. S. D. Deshmukh, “Model for Prediction of Temperature Distribution in Workpiece for Surface Grinding using FEA”, *International Journal of Advanced Research in Engineering & Technology (IJARET)*, Volume 3, Issue 2, 2012, pp. 207 - 213, ISSN Print: 0976-6480, ISSN Online: 0976-6499.